Available online at www.sciencedirect.com
ScienceDirect
Journal of Hazardous Materials 157 (2008) 57–63
Journal of Hazardous Materials
www.elsevier.com/locate/jhazmat

Visible light induced electron transfer process over nitrogen doped TiO_2 nanocrystals prepared by oxidation of titanium nitride

Zhongbiao Wu, Fan Dong, Weirong Zhao *, Sen Guo

Department of Environmental Engineering, Zhejiang University, Hangzhou 310027, China

Received 4 December 2007; received in revised form 17 December 2007; accepted 19 December 2007
Available online 31 December 2007

Abstract

Nitrogen doped TiO_2 nanocrystals with anatase and rutile mixed phases were prepared by incomplete oxidation of titanium nitride at different temperatures. The as-prepared samples were characterized by X-ray diffraction (XRD), transmission electron microscopy (TEM), high resolution transmission electron microscopy (HRTEM), core level X-ray photoelectron spectroscopy (CL XPS), valence band X-ray photoelectron spectroscopy (VB XPS), UV–vis diffuse reflectance spectra (UV–vis DRS), and visible light excited photoluminescence (PL). The photocatalytic activity was evaluated for photocatalytic degradation of toluene in gas phase under visible light irradiation. The visible light absorption and photoactivities of these nitrogen doped TiO_2 nanocrystals can be clearly attributed to the change of the additional electronic (N^-) states above the valence band of TiO_2 modified by N dopant as revealed by the VB XPS and visible light induced PL. A band gap structure model was established to explain the electron transfer process over nitrogen doped TiO_2 nanocrystals under visible light irradiation, which was consistent with the previous theoretical and experimental results. This model can also be applied to understand visible light induced photocatalysis over other nonmetal doped TiO_2.

Keywords: Valence band X-ray photoelectron spectroscopy; Visible light induced photoluminescence; Nitrogen doping; Photocatalytic activity; Toluene

1. Introduction

TiO_2 nanomaterial is one of the most promising photocatalysts due to its high efficiency, good stability, nontoxicity, and availability, which makes it attractive for the degradation of environmental organic pollutants [1,2]. However, TiO_2 only becomes active under irradiation with ultraviolet (UV) light. Thus, many efforts have been devoted recently to improve the optical response of TiO_2 in the visible region. Doping TiO_2 with different elements such as nitrogen [3,4], carbon [5,6], and sulfur [7,8] has displayed promising results in visible light (>400 nm) induced photocatalysis.

Nitrogen doping of TiO_2 can be achieved by one of the following techniques: (1) sputtering followed by annealing under a controlled atmosphere [3], (2) annealing pure TiO_2 powders under dopant-generating atmospheres (such as NH_3) [9], (3) solution-based strategies such as precipitation [10,11], sol–gel [12], and solvothermal treatment [13], and (4) direct oxidation of the dopant-containing titanium precursors (such as TiN) at proper temperatures [14]. Except for method (4), other methods usually involve complex reactions, resulting in various nitrogen species in the final photocatalysts, which makes it difficult to clarify the effect of nitrogen doping on the band gap structure experimentally.

It is well known that titanium nitride (TiN) can be oxidized to TiO_2 by high temperature annealing in air or oxygen atmosphere [14,15]. TiN is a metallic conductor with a partially filled band and a chemical bond of simultaneously metallic, covalent, and ionic characters. And thus the simple process of incomplete oxidation of this material provides an attractive technique to prepare the nitrogen doped TiO_2, which is convenient for investigating the effect of nitrogen doping. Oxidation of TiN to prepare nitrogen doped TiO_2 has been reported [14], and little is known about its electronic structure and visible light properties. Besides, there is little direct experimental evidence on the electronic origin for the visible-light absorption properties and photoactivities of nitrogen doped TiO_2 by oxidation of TiN.

Here, nitrogen doped TiO_2 nanocrystals are prepared by incomplete oxidizing TiN at different temperatures in air. These

* Corresponding author. Tel.: +86 571 8795 1571; fax: +86 571 8795 1571.
E-mail address: weirong@mail.hz.zj.cn (W. Zhao).

0304-3894/$ – see front matter © 2007 Elsevier B.V. All rights reserved.
doi:10.1016/j.jhazmat.2007.12.079

catalysts show high visible light photocatalytic activities for degradation of toluene in gas phase. Different techniques are employed to investigate the chemical and structure features of the prepared catalysts, especially the valence band spectroscopy (VB XPS) and visible light induced photoluminescence (PL), which reveal the electronic origin of the visible light absorption properties and photoactivities of the nitrogen doped TiO_2 nanocrystals. A band gap structure model is then established to explain the visible light induced electron transfer process over the prepared nitrogen doped TiO_2 nanocrystals.

2. Experimental

2.1. Preparation of photocatalysts

The titanium nitride (TiN) was obtained from Hefei Kaier Nano Company (China) and used as obtained. The commercially available TiO_2 (Degussa P25) was obtained from Degussa Chemical (Germany). The nitrogen doped titanium dioxide (TiO_2) nanocrystals were prepared by heating TiN at 450, 550 and 650 °C for 2 h in air, respectively. About 3.0 g TiN powder was loaded in a ceramic crucible, and then placed in the middle of muffle furnace, which was open to the atmosphere. The temperature was slowly ramped up and cooled down at a rate of 2 °C/min during the heating and cooling processes. After cooling to room temperature, the samples were taken out for further investigations. The as-prepared samples were labeled as N450, N550, and N650, respectively.

2.2. Characterization

The crystal phases of the sample were analyzed by X-ray diffraction with Cu Kα radiation (XRD: model D/max RA, Rigaku Co., Japan). The accelerating voltage and the applied current were 40 kV and 150 mA, respectively. X-ray photoelectron spectroscopy with Al Kα X-rays ($h\nu = 1486.6$ eV) radiation operated at 150 W (XPS: Thermo ESCALAB 250, USA) was used to investigate the surface properties and to probe the total density of the state (DOS) distribution in the valence band of the samples. The shift of the binding energy due to relative surface charging was corrected using the C1s level at 284.8 eV as an internal standard. The morphology, structure and grain size of the samples were examined by transmission electron microscopy (TEM: JEM-2010, Japan). The UV–vis absorbance spectra were obtained for the dry-pressed disk samples using a Scan UV–vis spectrophotometer (UV–vis DRS: TU-1901, China) equipped with an integrating sphere assembly, using $BaSO_4$ as reflectance sample. The spectra were recorded at room temperature in air ranged from 230 to 800 nm. The PL spectra were measured at room temperature with a fluorospectrophotometer (PL: Fluorolog-3-Tau, France) using a Xe lamp as excitation source. Nitrogen adsorption–desorption isotherms were obtained on a nitrogen adsorption apparatus (ASAP 2020, USA). All the samples were degassed at 200 °C prior to BET measurements. The Brunauer–Emmett–Teller (BET) specific surface area (S_{BET}) was determined by a multipoint BET method using the adsorption data in the relative pressure (P/P_0) range from 0.05 to 0.30.

2.3. Photocatalytic activity tests

Photocaytalytic degradation of toluene is chosen as the probe reaction to characterize the activity of the prepared samples, as toluene is a typical indoor pollutant [16,17]. The photocatalytic activity experiments of the as-prepared catalysts for the oxidation of toluene in air were performed at room temperature using a 1.8 L photocatalytic reactor. The catalyst was prepared by coating an ethanol suspension of the as-prepared catalyst onto a dish with diameter of 12.5 cm. The weight of catalyst used for each test was kept at 0.20 g. The dish containing catalyst was dried at 60 °C for 1 h to evaporate the ethanol and then cooled to room temperature before being used. After the catalyst-coated dish was placed in the reactor, a small amount of toluene was injected into the reactor with a micro-syringe. The analysis of toluene concentration in the reactor was conducted with a GC-FID (FULI 9790, China). The toluene vapor was allowed to reach adsorption equilibrium with the catalyst in the reactor prior to irradiation. The initial concentration of toluene after adsorption equilibrium was controlled at 150 mg/m^3. A 150 W Xe lamp was placed above the reactor as the light source. For visible light photocatalysis, a glass optical filter was inserted to cut off the short wavelength components ($\lambda < 425$ nm). The initial temperature was 25 ± 1 °C by cooling air. The initial relative humidity was controlled by a $CaCl_2$ dryer connected to the photoreactor.

The photocatalytic activity of the catalyst samples can be quantitatively evaluated by comparing the apparent reaction rate constants. The photocatalytic oxidation of toluene is a pseudo-first-order reaction and its kinetics may be expressed as follows: $\ln(C_0/C) = kt$ [18], where k is the apparent reaction rate constant, C_0 and C are the initial concentration and the reaction concentration of toluene, respectively.

3. Results and discussion

3.1. Phase structure and BET

TiN has a NaCl-like cubic structure and crystallize in the rock-salt structure, with N atoms occupying interstitial positions in a close-packed arrangement of Ti atoms [19]. This structure gives rise to strong metal to metal and metal to non-metal interactions.

Calcination temperatures have great influence on the phase structures and surface areas of photocatalysts [20,21]. Fig. 1 shows the X-ray diffraction (XRD) patterns of commercial TiN powders and the resultant nitrogen doped TiO_2 nanocrystals after heating at 450, 550, and 650 °C for 2 h in air, respectively. The TiN cubic structure was converted into the nitrogen doped TiO_2 nanocrstals with anatase and rutile mixed phases after heating.

The average crystalline sizes of anatase and rutile in the samples were calculated by applying the Debye–Scherrer equation [22]. The phase contents of the samples can be estimated from

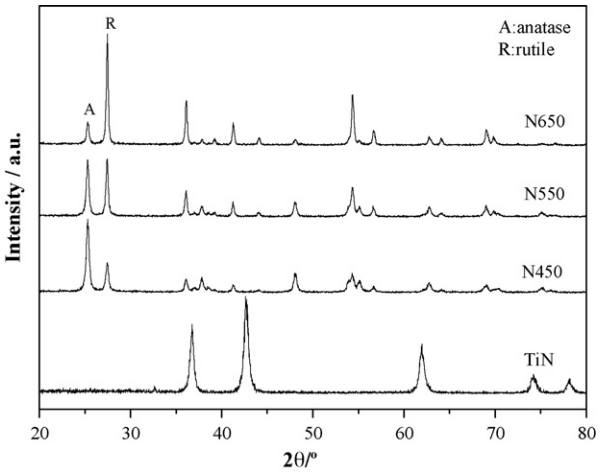

Fig. 1. X-ray diffraction patterns of N450, N550 and N650 samples and TiN.

the respective XRD peak intensities using the following equation [22]:

$$f_A = \left(1 + \frac{1}{K}\frac{I_R}{I_A}\right)^{-1} \quad (1)$$

where f_A is the fraction of anatase phase in the powder, and I_A and I_R are the X-ray intensities of the anatase (1 0 1) and rutile (1 1 0) diffraction peaks, respectively. The contents of the anatase phases in the samples were shown in Table 1.

It can be seen from Table 1 that the crystal size of both anatase and rutile increased with increasing calcination temperatures. The anatase molar ratio and specific surface area (S_{BET}) decreased with the increasing calcination temperatures.

The structure of N-doped TiO_2 powders was further investigated by TEM and HRTEM images as shown in Fig. 2. It can be seen from Fig. 2a and b that well-dispersed nanometer sized nitrogen doped TiO_2 nanocrystals existed as a mix of two different sizes, 27 ± 2 and 35 ± 2 nm, respectively. The smaller one can be ascribed to anatase crystal and the bigger one to rutile, which was consistent to the calculated result from XRD. High-resolution transmission electron microscopy (HRTEM) images (Fig. 2c and d) showed that nitrogen doped nanocrystals had cubic shapes and were highly crystallized with well-resolved lattice structure. The observed spacing between the lattice planes of the sample was obtained as 0.350 and 0.322 nm for (1 0 1) plane of the anatase and (1 1 0) plane of the rutile crystal, respectively. The crystal lattice was very clear, indicating no obvious defects. However, O vacancies (O_V) as one kind of defect might exist in the samples due to the charge imbalance caused by anionic nitrogen (N^-) [23].

3.2. XPS analysis

X-ray photoelectron spectroscopy (XPS) is usually used to determine the chemical composition of the materials, electronic structure as well as surface properties. To investigate the chemical states and the concentration of nitrogen atoms incorporated into the TiO_2 photocatalyst, the core level X-ray photoelectron spectroscopy (CL XPS) of N1s binding energy was measured.

Fig. 3 shows the CL XPS spectra for the N1s region of N-doped TiO_2 nanocrystals under different calcination temperatures. In general, the peak of N1s from the CL XPS spectra mostly lies in the range of 396–404 eV, and there are different spectral features with different preparation methods and conditions [3,4,9,10–15,24,25]. It can be seen that N1s peak at 397 eV [15] of TiN did not appear, and a broad peak from 398 to 403 eV appeared, which centered at around 400 eV. The atomic nitrogen content of sample N450, N550 and N650 was calculated to be 0.8, 0.6, 0.5%, respectively, indicating that the content of nitrogen maintained decreased when the calcination temperature increased. In the heating process, N was replaced by O and removed to form N_2. Therefore, in the incomplete oxidation process, partial Ti–N bonds were retained, and new N–Ti–O structure formed. This was further confirmed by the bonding energy of N1s of the as-prepared samples, which was proved to be N–Ti–O structure [24,25], a typical feature of substitutional N state.

It has been reported that nitrogen doping could enhance the visible light absorption and modify the band gap structure of TiO_2. In order to investigate the nature of the band structure, we obtained the valence band (VB) XPS, which can directly probe the total density of the state (DOS) distribution in the valence band [26], using a photon energy of 1486.6 eV.

Direct evidence on the modification of the TiO_2 valence band caused by the nitrogen dopant is obtained from the VB XPS. It can be seen from Fig. 4 that additional electronic states below 3.05 eV were observed above the valence band edge as compared to pure TiO_2. These states can be attributed to the N2p orbitals in nitrogen doped TiO_2. This evidence directly supported the theoretical DFT predictions and experimental results [3,27,28] that the nitrogen dopant provided additional electronic states above the valence band edge of pure TiO_2 and the substitutional N states lie above the valence band. These additional states were directly responsible for the visible-light absorption and photoactivities of the nitrogen doped TiO_2 nanocrystals [3,27,28].

3.3. UV–vis DRS and PL

Each nitrogen-doped sample exhibited a pale yellow color. Fig. 5 shows the diffuse reflection spectra of the samples

Table 1
Physicochemical properties of the as-prepared samples and their photoactivities

Sample	Anatase (nm)	Rutile (nm)	f_A (%)	S_{BET} (m^2/g)	Abs at 450 nm	$k \times 10^3$ (min^{-1})	$k/S_{BET} \times 10^4$ (min^{-1}/m^2 g)
N450	24.5	27.0	67.8	62.8	0.074	10.5	1.67
N550	27.9	34.9	47.3	48.2	0.045	5.3	1.10
N650	31.6	43.7	18.8	30.0	0.021	0.7	0.23

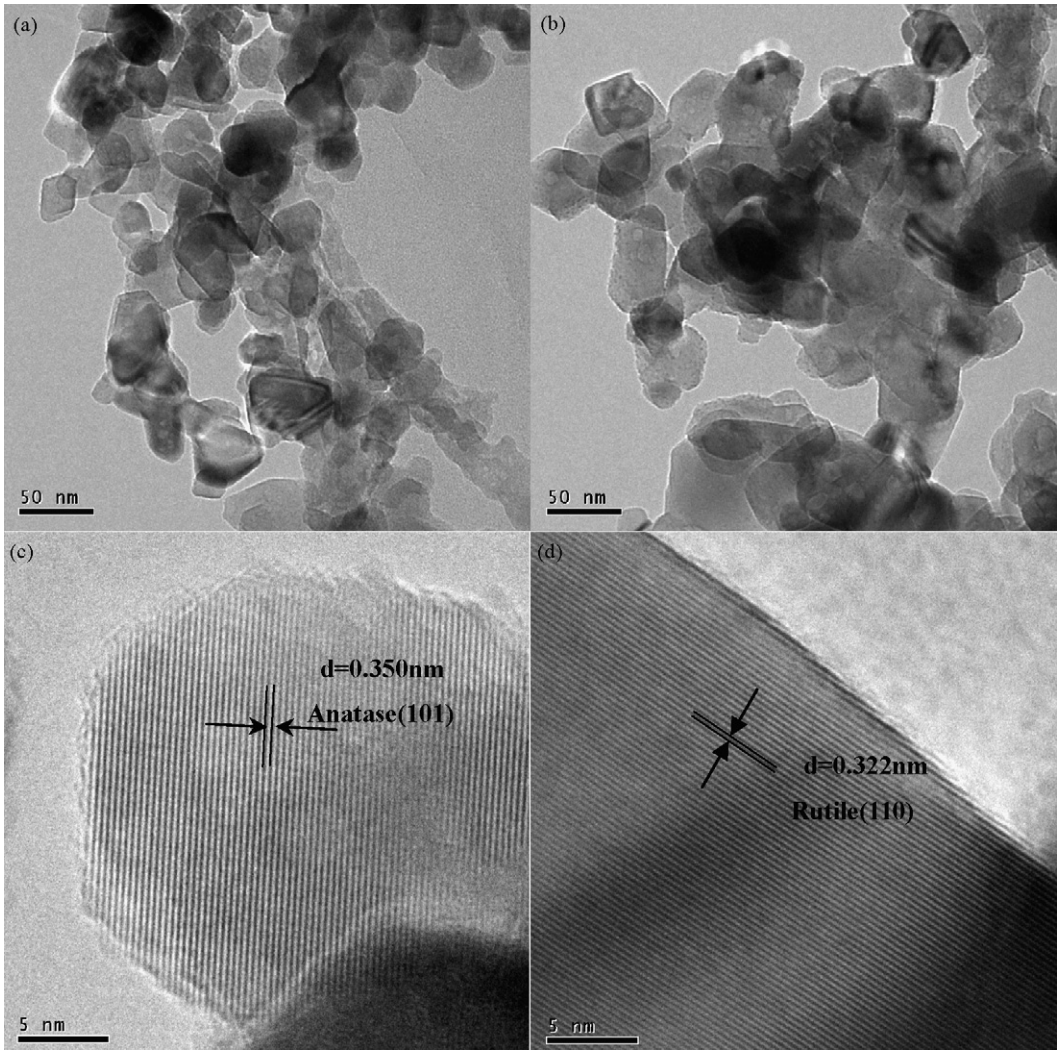

Fig. 2. TEM and HRTEM images of sample N550.

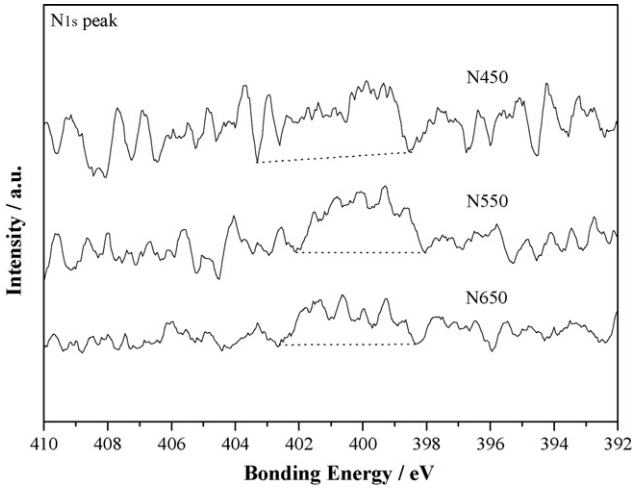

Fig. 3. Core level XPS spectra of N1s region of the N450, N550 and N650 samples.

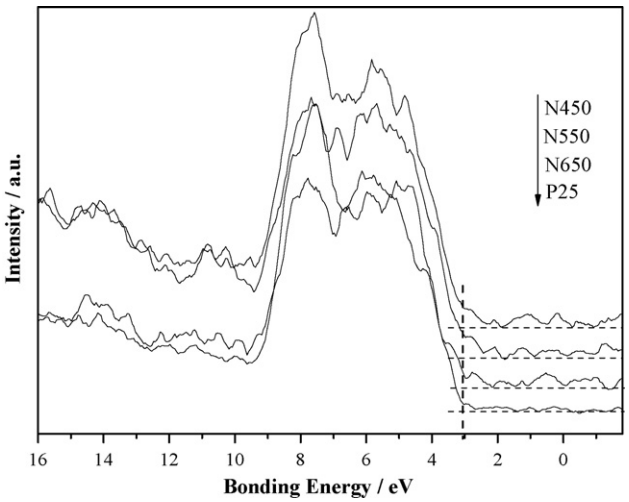

Fig. 4. Valence band XPS spectra of N450, N550, N650 samples and P25.

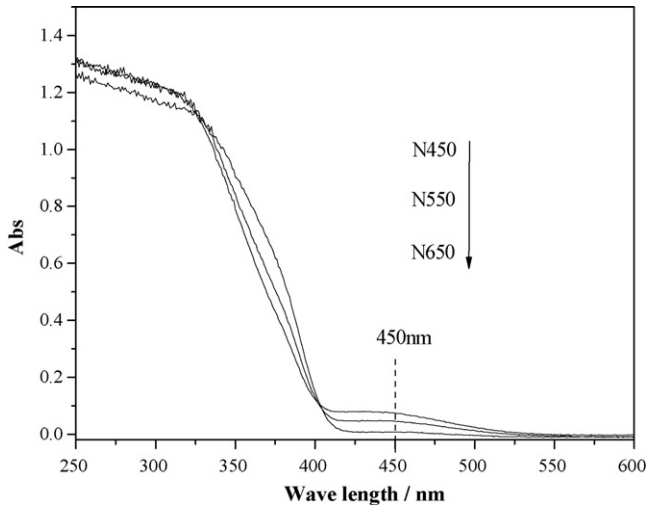

Fig. 5. UV–vis diffuse reflectance spectra of N450, N550 and N650 samples.

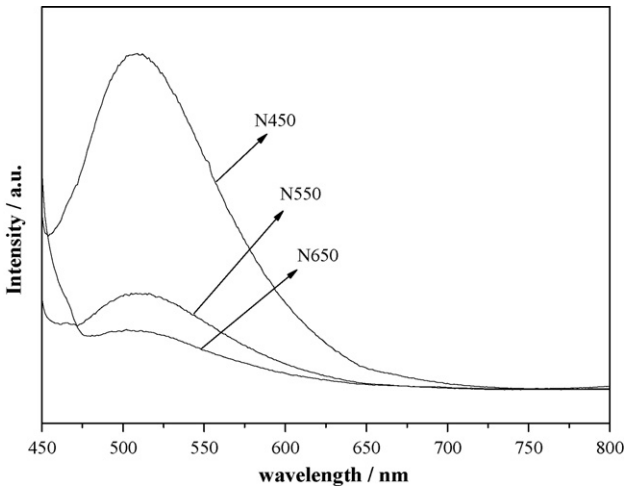

Fig. 6. Photoluminescence spectra of N450, N550 and N650 samples (excitation source: 425 nm).

calcined at different temperatures. A significant increase in the absorption at wavelengths shorter than 400 nm can be assigned to the intrinsic band gap absorption of TiO_2. The absorption spectra of the N-doped TiO_2 nanocrystals showed absorption in the visible light region due to the formation of new electronic state above valence band caused by nitrogen doping [3,27,28], as evidenced by VB XPS. As the calcination temperature increased, the absorption of the as-prepared samples decreased in the visible region (at 450 nm). This can be attributed to the reduction in the nitrogen content of the doped samples due to higher calcination temperatures.

PL emission spectra have been widely used to investigate the efficiency of charge carrier trapping, migration, and transfer in order to understand the fate of electron–hole pairs in semiconductor particles since PL emission results from the recombination of free carriers [29,30]. Many studies have reported PL emissions of TiO_2 based photocatalyst when the wavelength of excitation source located at UV region [29,30]. To the best of our knowledge, there is no report on exciting nitrogen doped TiO_2 with visible light.

Fig. 6 shows the room-temperature PL spectra of TiO_2 nanocrystals doped with different amounts of N using the excitation light of 425 nm. The energy of the used excitation light is enough to promote electronic transitions from the additional electronic states N^- to the conduction band of N-doped TiO_2 according to the above UV–vis spectra. All the samples can exhibit an obvious PL signal with a similar curve shape at the wavelength range from 400 to 550 nm. The PL intensity of the samples decreased with increasing calcination temperatures. The different quenching of the PL intensities was attributed to different content of nitrogen doped into TiO_2. This will be discussed in the following section.

3.4. Band gap structure

It was generally accepted that nitrogen doping can form a new electronic states (N^- state) just above the valence band, making TiO_2 absorb visible light [28], which was further confirmed experimentally by VB XPS (Fig. 4) and visible light induced PL (Fig. 6). It was proved by DFT calculations that N-doping favored the formation of O vacancy (sub-band level O_V), which was experimentally found to be about 0.8 eV below the bottom of the conduction band [28,31]. The O vacancies of nanosized semiconductor easily capture or bind photoinduced electrons [32], which have been proved by the electronic spin resonance method [33]. Hence, the larger the O_V content is, the stronger the PL intensity possibly is.

In order to understand the electron transfer process over the prepared nitrogen doped TiO_2 nanocrystals under visible light illumination, a schematic model of band gap structure was established, as illustrated in Fig. 7. The energy of the visible light (425 nm) is not sufficient to excite electrons from the valence band (VB), as the intrinsic band gap of TiO_2 corresponds to 387 nm for anatase or 410 nm for rutile, i.e., the process A cannot occur (Fig. 7). After nitrogen doping, the electron (e^-) can be excited from the N^- impurity level to the conduction band

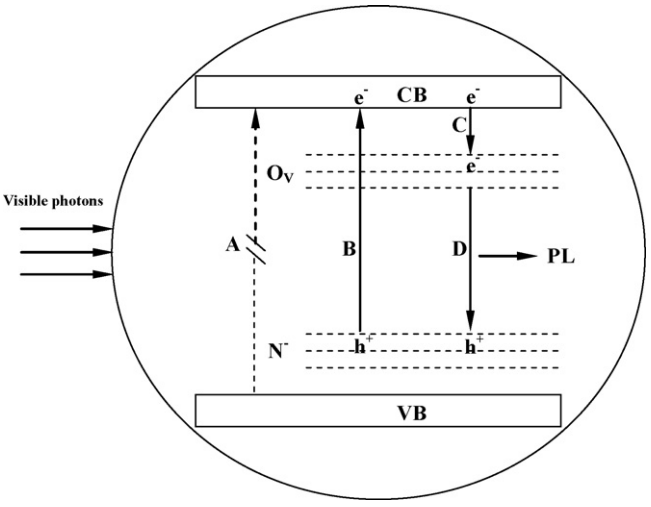

Fig. 7. Schematic diagram of electron transfer process over N-doped TiO_2 nanocrystals under visible light irradiation.

(CB), as the process B illustrates. Next, the exited electrons are trapped or bound to the level of sub-band (O_V) (process C). Finally, the photoinduced electrons in the O_V state can recombine with the holes (h^+) in the N impurity level (process D) to give rise to PL signals (Eqs. (2) and (3)).

$$O_V + e_{CB}{}^- \rightarrow O_V{}^- \quad (2)$$

$$O_V{}^- + h^+ \rightarrow O_V + PL \quad (3)$$

The different quenching of the PL intensities of the samples was attributed to different content of nitrogen. As the O_V was caused by nitrogen doping, it was reasonable to accept that the amount of O_V sites was dependent on the content of N^-. When the calcination temperature increased, the doping content of nitrogen decreased, thus the content of O_V formed decreased and less photo-induced electrons can be trapped by the O_V. This will result in the decrease of PL intensity with increasing temperatures (Fig. 6).

As the mechanism of nonmetal doping is somewhat similar [27,34], this model may be helpful to understand the mechanism of visible light photocatalysis over other nonmetal (such as boron or carbon) doped TiO_2 photocatalyst.

3.5. Visible light photocatalytic activity

To compare the photocatalytic activity of the as-prepared photocatalysts prepared under different conditions, photodegradation of toluene in gas phase as a test reaction was performed.

The results of the photocatalytic activities are shown in Fig. 8, where C_0 and C are the initial concentration after the equilibrium and the reaction concentration of toluene, respectively. Under visible light irradiation, holes in the N^-state and electrons in conduction band were generated. The holes and electrons will react with OH^- and molecule O_2 on the catalyst surface to form $^{\bullet}OH$ and $O_2{}^-$ [1], respectively, by which toluene was minerlized completely.

When the calcination temperature increased from 450 to 650 °C, the photocatalytic reaction over the as-prepared samples becomes slower (the value of k/S_{BET} varied from 1.67 to 0.23×10^{-4} min^{-1}/m^2 g), as shown in Table 1. It is interesting to mention that the activity order of the samples doped with different amounts of N are in good agreement with their corresponding PL intensity order, in other words, the stronger the PL signal, the higher the photocatalytic activity. It was different from reported results that lower PL intensity of photocatalysts corresponded to the higher photocatalytic activity due to the higher separation rate of photo-induced electrons and holes [35–37]. These results were mainly attributed to the effect of O vacancies on the different quenching of the PL as previously mentioned. The increase in the O vacancies amount was favorable for the increase in the PL intensity and advantageous to facilitate the separation of photoinduced charge carriers so as to enhance the activity.

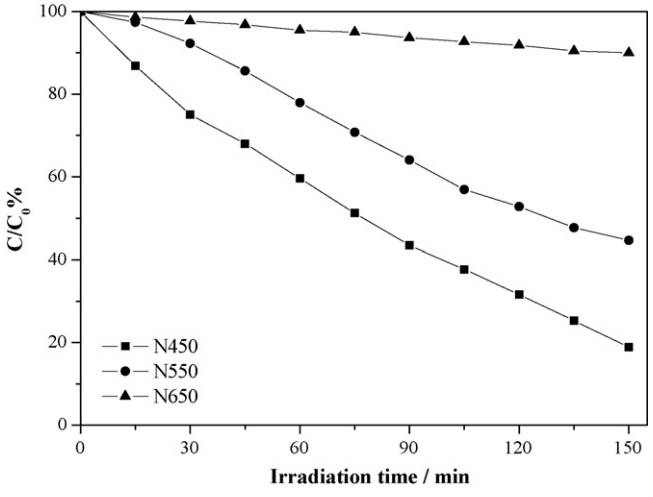

Fig. 8. Toluene degradation of N450, N550 and N650 samples under visible light irradiation (425 nm < λ <700 nm).

4. Conclusions

Nitrogen doped TiO_2 nanocrystals can be developed directly from a single inorganic precursor by incomplete oxidation of TiN at different temperatures. The visible light photocatalytic activities of the prepared catalysts for degradation of toluene in gas phase were dependent on the doped nitrogen content. Valence band XPS and visible light exited PL clearly revealed the additional electronic states in the band gap caused by the nitrogen dopant, compared to pure TiO_2. The additional N^- states were responsible for the electronic origin for the visible-light absorption and photocatalytic properties of the nitrogen-doped TiO_2. The visible light induced electron transfer process over the nitrogen-doped TiO_2 can be described by the established physical model of band gap structure. This process involved the following steps: (1) generation of electrons from the N^- impurity level to the conduction band under visible light irradiation, (2) trapping of exited electrons by the level of sub-band (O_V), (3) recombination of the photoinduced electrons with the holes in the N impurity level to give rise to PL signal. This model can be used to understand visible light induced process and other nonmetal doped TiO_2.

Acknowledgements

This research was financially supported by the Chinese Key Technology R&D Program of the Eleventh Five-year Plan (2006BAJ02A08), the Natural Science Fundation of Zhejiang Province (Y50596) and the Hangzhou Science & Technology Development Program (20061133B27).

References

[1] X.B. Chen, S.S. Mao, Titanium dioxide nanomaterials: synthesis, properties, modifications, and applications, Chem. Rev. 107 (2007) 2891–2959.
[2] T. Aarthi, P. Narahari, G. Madras, Photocatalytic degradation of Azure and Sudan dyes using nano TiO_2, J. Hazard. Mater. 149 (2007) 725–734.
[3] R. Asahi, T. Morikawa, T. Ohwaki, K. Aoki, Y. Taga, Visible-light photocatalysis in nitrogen-doped titanium oxides, Science 293 (2001) 269–271.
[4] Y. Wang, C.X. Feng, Z.S. Jin, J.W. Zhang, H.J. Yang, S.L. Zhang, A novel N-doped TiO_2 with high visible light photocatalytic activity, J. Mol. Catal. A: Chem. 260 (2006) 1–3.

[5] S. Sakthivel, H. Kisch, Daylight photocatalysis by carbon-modified TiO_2, Angew. Chem. Int. Ed. 42 (2003) 4908–4911.
[6] C.S. Kuo, Y.H. Tseng, C.H. Huang, Y.Y. Li, Carbon-containing nano-titania prepared by chemical vapor deposition and its visible-light-responsive photocatalytic activity, J. Mol. Catal. A: Chem. 270 (2007) 93–100.
[7] T. Umebayashi, T. Yamaki, S. Tanala, K. Asai, Visible light-induced degradation of methylene blue on S-doped TiO_2, Chem. Lett. 32 (2003) 330–331.
[8] J.C. Yu, W.K. Ho, J.G. Yu, H. Yip, P.K. Wong, J.C. Zhao, Efficient visible-light-induced photocatalytic disinfection on sulfur-doped nanocrystalline titania, Environ. Sci. Technol. 39 (2005) 1175–1179.
[9] H. Irie, Y. Watanabe, K. Hashimoto, Nitrogen-concentration dependence on photocatalytic activity of $TiO_{2-x}N_x$ powders, J. Phys. Chem. B 107 (2003) 5483–5486.
[10] J.G. Yu, M.H. Zhou, B. Cheng, X.J. Zhao, Preparation, characterization and photocatalytic activity of in situ N,S-codoped TiO_2 powders, J. Mol. Catal. A: Chem. 246 (2006) 176–184.
[11] Y.Q. Wang, X.J. Yu, D.Z. Sun, Synthesis, characterization, and photocatalytic activity of $TiO_{2-x}N_x$ nanocatalyst, J. Hazard. Mater. 144 (2007) 328–333.
[12] J.L. Gole, J.D. Stout, C. Burda, Y.B. Lou, X.B. Chen, Highly efficient formation of visible light tunable $TiO_{2-x}N_x$ photocatalysts and their transformation at the nanoscale, J. Phys. Chem. B 108 (2004) 1230–1240.
[13] Y. Aita, M. Komatsu, S. Yin, T. Sato, Phase-compositional control and visible light photocatalytic activity of nitrogen-doped titania via solvothermal process, J. Solid State Chem. 177 (2004) 3235–3238.
[14] T. Morikawa, R. Asahi, T. Ohwaki, K. Aoki, Y. Taga, Band-gap narrowing of titanium dioxide by nitrogen doping, Jpn. J. Appl. Phys., Part 2 40 (2001) L561–L563.
[15] N.C. Saha, H.G. Tompkins, Titanium nitride oxidation chemistry: an X-ray photoelectron spectroscopy study, J. Appl. Phys. 72 (1992) 3072–3079.
[16] R. Yang, Y.P. Zhang, Q.J. Xu, J.H. Mo, A mass transfer based method for measuring the reaction coefficients of a photocatalyst, Atmos. Environ. 41 (2007) 1221–1229.
[17] Y.P. Zhang, R. Yang, Q.J. Xu, J.H. Mo, Characteristics of photocatalytic oxidation of toluene, benzene, and their mixture, J. Air Waste Manage. Assoc. 57 (2007) 94–101.
[18] J.G. Yu, G.H. Wang, B. Cheng, M.H. Zhou, Effects of hydrothermal temperature and time on the photocatalytic activity and microstructures of bimodal mesoporous TiO_2 powders, Appl. Catal. B 69 (2007) 171–180.
[19] S.V. Didziulis, J.R. Lince, T.B. Stewart, E.A. Eklund, Photoelectron spectroscopic studies of the electronic structure and bonding in TiC and TiN, Inorg. Chem. 33 (1994) 1979–1991.
[20] J.G. Yu, L.J. Zhang, B. Cheng, Y.R. Su, Hydrothermal preparation and photocatalytic activity of hierarchically sponge-like macro-/mesoporous titania, J. Phys. Chem. C 111 (2007) 10582–10589.
[21] J.G. Yu, Y.R. Su, B. Cheng, Template-free fabrication and enhanced photocatalytic activity of hierarchical macro-/mesoporous titania, Adv. Funct. Mater. 17 (2007) 1984–1990.
[22] M.C. Yan, F. Chen, J.L. Zhang, M. Anpo, Preparation of controllable crystalline titania and study on the photocatalytic properties, J. Phys. Chem. B 109 (2005) 8673–8678.
[23] H.W. Xu, Y.L. Su, M.L. Balmer, A. Navrotsky, A new series of oxygen-deficient perovskites in the $NaTi_xNb_{1-x}O_{3-0.5x}$ system: synthesis, crystal chemistry, and energetics, Chem. Mater. 15 (2003) 1872–1878.
[24] X.B. Chen, C. Burda, Photoelectron spectroscopic investigation of nitrogen-doped titania nanoparticles, J. Phys. Chem. B 108 (2004) 15446–15449.
[25] Y. Cong, J.L. Zhang, F. Chen, M. Anpo, Synthesis and characterization of nitrogen-doped TiO_2 nanophotocatalyst with high visible light activity, J. Phys. Chem. C 111 (2007) 6976–6982.
[26] Y.Y. Mi, Z. Yu, S.J. Wang, X.Y. Gao, A.T.S. Wee, C.K. Ong, C.H.A. Huan, Thermal stability of nitrogen-doped $SrTiO_3$ films: electronic and optical properties studies, J. Appl. Phys. 101 (2007), Art. No. 063708.
[27] C. Di Valentin, G. Pacchioni, A. Slloni, S. Livraghi, E. Giamello, Characterization of paramagnetic species in N-doped TiO_2 powders by EPR spectroscopy and DFT calculations, J. Phys. Chem. B 109 (2005) 11414–11419.
[28] S. Livraghi, M.C. Paganini, E. Giamello, A. Selloni, C. Di Valentin, G. Pacchioni, Origin of photoactivity of nitrogen-doped titanium dioxide under visible light, J. Am. Chem. Soc. 128 (2006) 15666–15671.
[29] F.B. Li, X.Z. Li, The enhancement of photodegradation efficiency using Pt-TiO_2 catalyst, Chemosphere 48 (2002) 1103–1111.
[30] L.Q. Jing, Y.C. Qu, B.Q. Wang, S.D. Li, B.J. Jiang, L.B. Yang, W. Fu, H.G. Fu, J.Z. Sun, Review of photoluminescence performance of nano-sized semiconductor materials and its relationships with photocatalytic activity, Sol. Energy Mater. Sol. Cells 90 (2006) 1773–1787.
[31] M.A. Henderson, W.S. Epling, C.H.F. Peden, C.L. Perkins, Insights into photoexcited electron scavenging processes on TiO_2 obtained from studies of the reaction of O_2 with OH groups adsorbed at electronic defects on TiO_2(1 1 0), J. Phys. Chem. B 107 (2003) 534–545.
[32] L.Q. Jing, B.F. Xin, F.L. Yuan, L.P. Xue, B.X. Wang, H.G. Fu, Effects of surface oxygen vacancies on photophysical and photochemical processes of Zn-doped TiO_2 nanoparticles and their relationships, J. Phys. Chem. B 110 (2006) 17860–17865.
[33] L.Q. Jing, Z.L. Xu, X.J. Sun, J. Shang, W.M. Cai, The surface properties and photocatalytic activities of ZnO ultrafine particles, Appl. Surf. Sci. 180 (2001) 308–314.
[34] C. Di Valentin, G. Pacchioni, A. Selloni, Theory of carbon doping of titanium dioxide, Chem. Mater. 17 (2005) 6656–6665.
[35] J.G. Yu, H.G. Yu, B. Cheng, X.J. Zhao, J.C. Yu, W.K. Ho, The effect of calcination temperature on the surface microstructure and photocatalytic activity of TiO_2 thin films prepared by liquid phase deposition, J. Phys. Chem. B 107 (2003) 13871–13879.
[36] X.Z. Li, F.B. Li, C.L. Yang, W.K. Ge, Photocatalytic activity of WO_x-TiO_2 under visible light irradiation, J. Photochem. Photobiol. A: Chem. 141 (2001) 209–217.
[37] J.C. Yu, J.G. Yu, W.K. Ho, Z.T. Jiang, L.Z. Zhang, Effects of F^- doping on the photocatalytic activity and microstructures of nanocrystalline TiO_2 powders, Chem. Mater. 14 (2002) 3808–3816.